JOURNAL OF VIROLOGY, Dec. 1993, p. 7215–7222
0022-538X/93/127215-08$02.00/0

Vol. 67, No. 12

Three Different Cellular Proteins Bind to Complementary Sites on the 5′-End-Positive and 3′-End-Negative Strands of Mouse Hepatitis Virus RNA

TETSUYA FURUYA[1] AND MICHAEL M. C. LAI[1,2]*

Howard Hughes Medical Institute[2] and Department of Microbiology,[1] School of Medicine, University of Southern California, Los Angeles, California 90033-1054*

Received 4 June 1993/Accepted 10 September 1993

The termini of viral genomic RNA and its complementary strand are important in the initiation of viral RNA replication, which probably involves both viral and cellular proteins. To detect the possible cellular proteins involved in the replication of mouse hepatitis virus RNA, we performed RNA-protein binding studies with RNAs representing both the 5′ and 3′ ends of the viral genomic RNA and the 3′ end of the negative-strand complementary RNA. Gel-retardation assays showed that both the 5′-end-positive- and 3′-end-negative-strand RNA formed an RNA-protein complex with cellular proteins from the uninfected cells. UV cross-linking experiments further identified a 55-kDa protein bound to the 5′ end of the positive-strand viral genomic RNA and two proteins 35 and 38 kDa in size bound to the 3′ end of the negative-strand cRNA. The results of the competition assay confirmed the specificity of this RNA-protein binding. No proteins were found to bind to the 3′ end of the viral genomic RNA under the same conditions. The binding site of the 55-kDa protein was mapped within the 56-nucleotide region from nucleotides 56 to 112 from the 5′ end of the positive-strand RNA, and the 35- and 38-kDa proteins bound to the complementary region on the negative-strand RNA. The 38-kDa protein was detected only in DBT cells but was not detected in HeLa or COS cells, while the 35-kDa protein was found in all three cell types. The juxtaposition of the different cellular proteins on the complementary sites near the ends of the positive- and negative-strand RNAs suggests that these proteins may interact with each other and play a role in mouse hepatitis virus RNA replication.

Mouse hepatitis virus (MHV), a coronavirus prototype, contains a positive-sense single-stranded RNA genome 31 kb in size (16, 23). In infected cells, the viral genomic RNA is transcribed into negative-strand RNA (25), which in turn is used to transcribe seven to eight mRNAs. These mRNAs have a nested-set 3′-coterminal structure, and the 5′ end of each mRNA contains a 60- to 70-nucleotide (nt) leader sequence, which is identical among all the mRNAs and genomic RNA (14, 15, 31). It has been shown that the leader RNA is important for the regulation and initiation of transcription of subgenomic mRNAs (2, 14, 30).

The RNA sequences required for the transcription of MHV subgenomic mRNAs include both the 5′ end of the genomic RNA (i.e., the region containing the leader sequence) and the intergenic sequences (i.e., the transcription initiation sites of subgenomic mRNAs [14]). The latter region requires as few as 8 core nt (11, 19), but the sequence in the former region required for transcription has not been precisely characterized. The sequence required for the replication of the full-length genomic RNA has also been partially characterized; at least for a defective interfering RNA, more than 800 nt of the 5′-end sequence and 400 nt of the 3′-end sequence of the genomic RNA are required for RNA replication (17). However, the protein composition of the transcription or replication machineries for viral RNA synthesis is largely unknown. Presumably, virus-specific RNA polymerase, which is encoded by gene 1 of the MHV genome (14), is responsible for both the replication and transcription of MHV RNA. Because an antibody specific for the viral nucleocapsid protein inhibited RNA synthesis (4), the nucleocapsid protein may also be a component of the transcription or replication machinery. In view of the multiple functions required for viral RNA synthesis, it would not be surprising that some host cellular factors also participate in MHV RNA synthesis.

Studies with other positive-stranded RNA viruses indeed suggested the possible involvement of host cellular factors in viral RNA replication. For example, deletion mutants in the 5′ end of Sindbis virus RNA often have different levels of viral RNA replication in chicken and mosquito cells, suggesting that host factors interact with this RNA region and affect viral RNA replication in different cells (22). Several cellular proteins have been found to bind to the 3′ end of the negative-strand RNA of the Sindbis virus genome (24). The RNA-protein complex formed between cellular proteins and a mutant viral RNA which contains a lethal mutation had a longer half-life than that of the wild-type RNA-protein complex (24), suggesting the functional significance of the RNA-protein binding. Also, in poliovirus, a cellular protein was found to bind to a cloverleaf structure, which is required for RNA replication, at the 5′ end of RNA (1). The sequence or structure of the 5′ end of viral genomic RNA is probably directly involved in the RNA synthesis of most of the positive-stranded RNA viruses. For example, sequences similar to the internal control regions 1 and 2 of tRNA genes are found in the 5′ end of the genomic RNAs of brome mosaic virus and other plant viruses (26). The internal control region 2-like sequence in brome mosaic virus RNA forms a stem-loop structure. Most surprisingly, mutations which disrupt this structure in the positive-strand RNA reduced positive-strand RNA synthesis dramatically, but mutations which disrupt only negative-strand structure did not

* Corresponding author.

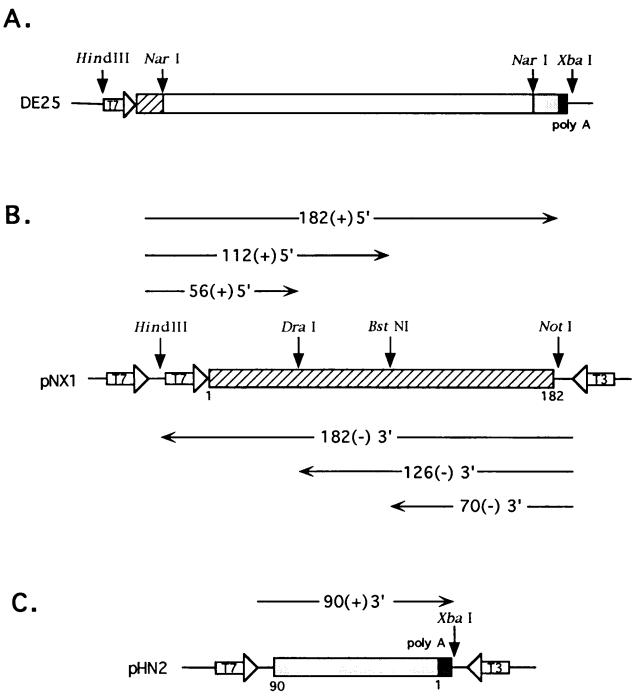

FIG. 1. Schematic diagrams of the structures of plasmids used in this study. Only the relevant sequences, including the MHV-specific sequences (in boxes) and T7 and T3 RNA polymerase promoters (large open arrows) are shown. pNX1 (B) and pHN2 (C) were derived from DE25 (A) (see Materials and Methods). Hatched boxes represent cDNA of 5′-end MHV RNA inserted into pNX1 (A and B). Shaded and solid boxes represent cDNA of 3′-end MHV RNA and poly(A) inserted into pHN2 (A and C). The numbers under the boxes denote nucleotide numbers in the MHV RNA sequence from the 5′ end (B) and the 3′ end (C), respectively (21).

significantly affect RNA synthesis (26), suggesting that the stem-loop structure at the 5′-end-positive-strand RNA is a promoter for genomic positive-strand RNA synthesis. All of these findings suggest potential roles in RNA replication of the 5′-end-positive- and 3′-end-negative-strand RNAs and of cellular proteins interacting with these regions.

In this study, we found that several different cellular proteins bind specifically to the complementary sites on the positive and negative strands of the 5′-end untranslated region (UTR) of MHV RNA. Some of the proteins are conserved among different cell lines. The possible roles of these proteins in viral RNA replication are discussed.

MATERIALS AND METHODS

Construction of plasmids. Plasmids pNX1 and pHN2 were used throughout this study to generate various RNA transcripts in vitro. These plasmids were derived from DE25/BSSK, which contained the complete cDNA sequence of DIssE RNA (21) in Bluescript SK(+) vector (Stratagene). The DE25/BSSK plasmid was made by releasing the DIssE cDNA from DE25 plasmid (20) by digestion with *Hin*dIII and *Xba*I and inserting the DIssE sequence into Bluescript SK(+) vector at the corresponding sites. DE25/BSSK was digested with *Nar*I-*Xba*I or *Nar*I-*Hin*dIII to remove most of the DIssE cDNA sequence (Fig. 1A), and the remaining sequence was blunt ended with T4 DNA polymerase and self-ligated to obtain pNX1 and *pHN2*, respectively. pNX1 contains 182 nt from the 5′ end of DIssE cDNA, which is flanked by two T7 promoters at the 5′ end and a T3 promoter at the 3′ end (Fig. 1B). It has 46 nt between the two T7 promoters and 43 nt of vector sequence downstream of the T3 promoter. Only the first T7 promoter was active in in vitro transcription reactions with T7 RNA polymerase (data not shown). pHN2 contains 90 nt from the 3′ end of DIssE cDNA, which is flanked by T7 promoter and 46 nt of vector sequence at the 5′ end, and a T3 promoter and 40 nt of vector sequence at the 3′ end (Fig. 1C).

In vitro RNA transcription. pNX1 was linearized with *Dra*I, *Bst*NI, and *Not*I and transcribed with T7 RNA polymerase to yield 56(+)5′, 112(+)5′, and 182(+)5′ RNA, respectively, which represent the 5′ end UTR of MHV genomic RNA (Fig. 1B). For the synthesis of negative-strand RNA, pNX1 was linearized with *Bst*NI, *Dra*I, and *Hin*dIII and transcribed with T3 RNA polymerase to generate 70(−)3′, 126(−)3′, and 182(−)3′ RNA, respectively, which represent the 3′ end of negative-strand RNA complementary to the 5′ end of MHV genomic RNA (Fig. 1B). For synthesis of the 3′ end of positive-strand RNA, pHN2 was linearized with *Xba*I and transcribed with T7 RNA polymerase to yield 90(+)3′, which represents the 3′ end of MHV genomic RNA including poly(A) (Fig. 1C). For synthesis of a nonspecific competitor, plasmid pTZ18U (U.S. Biochemicals) was linearized with *Pvu*II and transcribed with T7 RNA polymerase to generate a 149-nt RNA, which represents cloning sites and internal sequences of the vector. In vitro transcriptions were performed under the previously described conditions (33) at 37°C for 1 h. ^{32}P-labeled RNAs were obtained by transcription in the presence of 75 μCi of [α-^{32}P]UTP (3,000 Ci/mmol [ICN Biomedicals]), 12.5 μM UTP, and 500 μM (each) ATP, GTP, and CTP. Unlabeled RNAs were transcribed in the presence of 500 μM (each) ATP, GTP, CTP, and UTP. The transcribed RNAs were purified with a Sephadex G25 column equilibrated in STE buffer (10 mM Tris-HCl, 1 mM EDTA, 0.1 M NaCl [pH 7.5]) to remove unincorporated ribonucleotides.

Preparation of cytoplasmic extracts. DBT (9), COS-7 (8), and HeLa cells were grown in 15-cm-diameter dishes to confluence. Cells were washed with cold phosphate-buffered saline (PBS), scraped off the plates, and centrifuged at 1,500 × *g* for 10 min at 4°C. The cell pellets were resuspended in cold PBS (4.0×10^7 cells per ml), stored at −80°C, and thawed just before the experiments. Cytoplasmic extracts were prepared by a previously described method (29) with slight modifications. Briefly, 2.0×10^7 cells in an Eppendorf tube were pelleted by spinning for 15 s in a microcentrifuge. Cell pellets were resuspended in 400 μl of the extraction buffer (10 mM HEPES [*N*-2-hydroxyethylpiperazine-*N*′-2-ethanesulfonic acid, pH 7.9], 10 mM KCl, 0.1 mM EDTA, 1 mM dithiothreitol, 0.5 mM phenylmethylsulfonyl fluoride) at 4°C by gentle pipetting. Cells were allowed to swell on ice for 15 min. After addition of 25 μl of 10% Nonidet P-40, the mixture was vortexed vigorously for 10 s and centrifuged for 30 s in a microcentrifuge. The supernatant was collected, and the total protein concentration was determined with the Bio-Rad protein assay kit (Bio-Rad).

Gel-retardation assay of RNA-protein binding. The gel-retardation assay was carried out essentially as described previously (12) with slight modifications. Briefly, ^{32}P-labeled RNA (approximately 10^5 cpm, specific activity 2.5×10^9 cpm/μg) was mixed with different amounts of cellular extracts in 20 μl of the binding buffer (25 mM KCl, 5 mM HEPES [pH 7.5], 2 mM $MgCl_2$, 0.1 mM EDTA, 3.8% glycerol, 2 mM dithiothreitol). In competition assays, different amounts of unlabeled RNAs were lyophilized in Eppendorf tubes, resuspended together with a fixed amount of cellular extracts in the

binding buffer, and incubated at 30°C for 10 min prior to the addition of ^{32}P-labeled RNA. In all reaction mixtures, approximately 40 pg of ^{32}P-labeled RNA was used. The RNA-cellular extract mixture was incubated at 30°C for 10 min, followed by the addition of heparin to a final concentration of 1 mg/ml, and further incubated for 10 min. The reaction mixture was then mixed with one-fifth volume of 5× loading buffer (50% glycerol, 0.05% bromophenol blue, 0.05% xylene cyanol) and separated by electrophoresis on a 4% polyacrylamide gel made in 0.5× TBE (45 mM Tris-borate, 1 mM EDTA)–5% glycerol. The polyacrylamide gels had been preelectrophoresed at 200 V for 30 min prior to the loading of samples, and electrophoresis was performed at 200 V at room temperature until xylene cyanol reached a point one-third from the top of the gel.

UV cross-linking of RNA-protein complexes. The RNA-protein binding reaction was first carried out as described for the gel-retardation assay, except that the cell extracts were preincubated with yeast tRNA. Briefly, the cytoplasmic extracts from different cells were mixed with 10 μg of yeast tRNA and unlabeled competitor RNAs, if needed, in 20 μl of the binding buffer and incubated at 30°C for 10 min. Subsequently, 100 pg of ^{32}P-labeled RNA was added and the reaction mixture was incubated for an additional 10 min. The reaction mixture was then irradiated with UV light (254 nm [UV Stratalinker 2400; Stratagene]) on ice at a 14-cm distance for 10 min. After irradiation, RNase A was added to a final concentration of 1 mg/ml, and the mixture was incubated for 30 min at 37°C, boiled for 3 min in the sample buffer (10% glycerol, 5% β-mercaptoethanol, 3% sodium dodecyl sulfate [SDS], 62.5 mM Tris-HCl [pH 6.8]), and electrophoresed on a 12.5% polyacrylamide gel containing 0.1% SDS (13).

RESULTS

Binding of cellular proteins to MHV UTR RNA detected by gel-retardation assay. To determine whether any cellular proteins bind to the UTR of MHV RNA, we initially carried out gel-retardation assays of RNA-protein binding, using the cytoplasmic extracts from DBT cells and RNAs representing the 5′ end of positive-strand viral genomic RNA, the 3′ end of negative-strand cRNA, and the 3′ end of positive-strand viral genomic RNA. The sizes of RNAs used ranged from 90 to 182 nt plus various lengths of the vector sequence (see Materials and Methods). The 5′ end of negative-strand cRNA was not examined because of technical difficulty in plasmid construction and also because the 5′ end of negative-strand RNA is not expected to play a significant role in viral RNA synthesis (see Discussion). The results showed that a distinct RNA-protein complex of slower electrophoretic mobility was formed between the DBT cellular extract and both the 182(+)5′ and 182(−)3′ RNAs (Fig. 2). The amounts of the RNA-protein complexes increased when increasing amounts of the cellular extracts were used; correspondingly, the amounts of the free RNA probes decreased. In contrast, incubation of 90(+)3′ RNA with cellular extracts yielded only diffuse radioactivity, but no distinct RNA-protein complexes were detected (Fig. 2). The lack of protein binding to the 90(+)3′ RNA was confirmed by UV cross-linking studies (described below). Both 182(−)3′ and 90(+)3′ RNA preparations consisted of several RNA bands in the absence of the cellular extracts. They most likely represented different conformers or multimers of the same RNA, because only a single species was detected when the RNA transcript was examined by electrophoresis in agarose gels containing 6 M urea (data not shown). The 182(+)5′ RNA also consisted of a diffuse RNA band. This was likely also caused by RNA secondary structure, because it yielded a distinct band when analyzed by denaturing agarose gel electrophoresis (data not shown). Heparin, a negatively charged polymer, which had been reported to reduce nonspecific binding of proteins to RNA (5), was included in all of the RNA-protein binding assays. It did not affect the formation of the RNA-protein complex observed in this study.

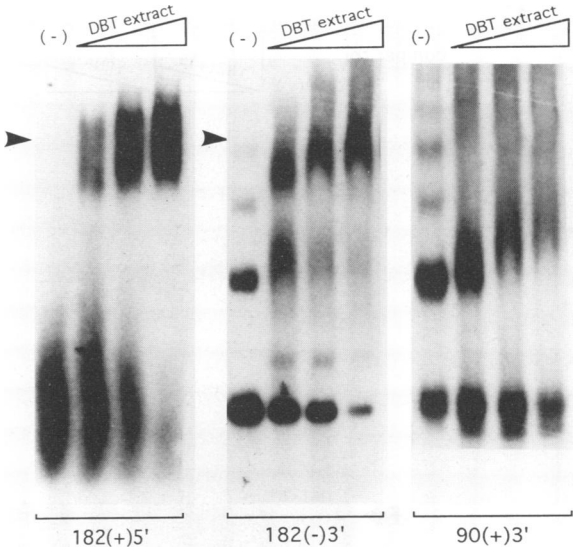

FIG. 2. Gel-retardation assay of RNA-protein complexes. ^{32}P-labeled 182(+)5′, 182(−)3′, and 90(+)3′ RNAs were each mixed with 1, 5, and 10 μg of cytoplasmic extracts from DBT cells. The arrowheads show protein-RNA complexes. In (−) lanes, no cellular extract was added. The RNA-protein complexes were separated in 4% polyacrylamide gels.

To examine the specificity of binding of the cellular proteins to UTR MHV RNAs, unlabeled specific and nonspecific RNAs were used as competitors for protein binding (Fig. 3). The results showed that, when increasing amounts of the unlabeled 182(+)5′ or 182(−)3′ RNAs were incubated with the cellular extracts prior to the addition of the ^{32}P-labeled respective RNAs, the RNA-protein complexes formed by both 182(+)5′ and 182(−)3′ RNAs proportionally decreased; in contrast, the comparable amounts of tRNA or vector RNA did not reduce the amounts of the RNA-protein complexes formed (Fig. 3). These results demonstrated that the binding of the cellular proteins to 182(+)5′ and 182(−)3′ RNAs was specific.

Identification of the bound cellular proteins by UV cross-linking. To identify the proteins which bound to the MHV UTR RNAs, ^{32}P-labeled RNAs were cross-linked to cellular proteins by UV irradiation and digested with RNase, and then the proteins were identified by SDS-polyacrylamide gel electrophoresis (PAGE). As shown in Fig. 4, 182(+)5′ RNA cross-linked to a protein approximately 55 kDa in size (arrowhead), which increased in amount when increasing amounts of cellular extracts were used. The 29-kDa band was probably an RNA fragment resistant to RNase, because this band was present even in the sample without cellular extract, and its amount decreased with increasing amounts of cellular extract. By comparison, 182(−)3′ RNA bound to two proteins of 35 and 38 kDa in size (Fig. 4, arrowheads). In some gels, a faint band approximately 90 kDa in size could also be detected, and its binding was specifically inhibited by the unlabeled homologous RNA (data not shown). The 90-kDa protein may be an

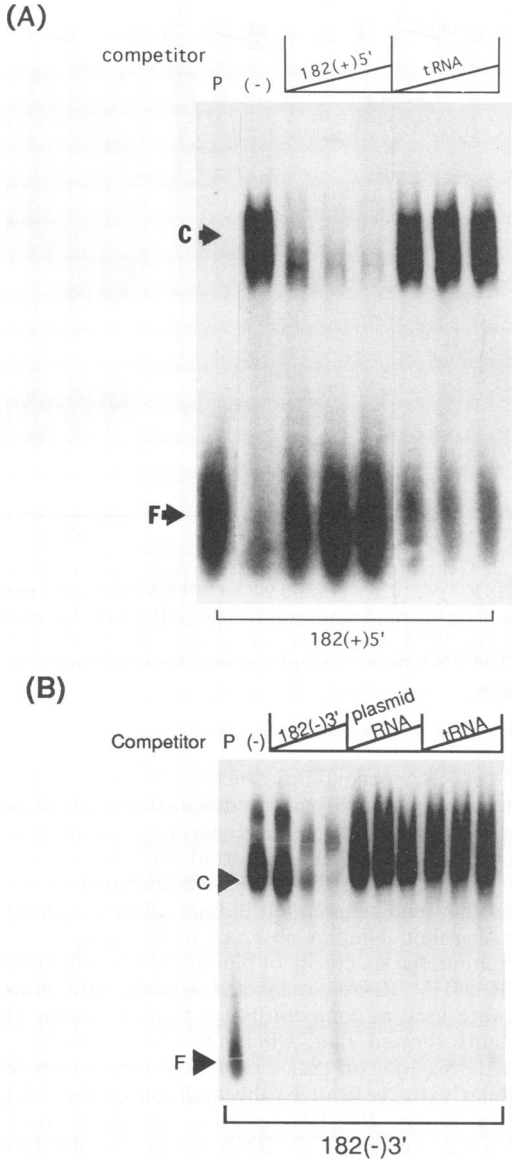

FIG. 3. Competition assays of RNA-protein binding. Approximately 5 μg of cellular extracts was incubated with various amounts of unlabeled RNAs for 10 min and then was incubated with the ^{32}P-labeled homologous RNAs. The unlabeled RNAs used represented 80-, 160-, and 320-fold excess over the labeled RNA. Corresponding amounts of unlabeled yeast tRNA or plasmid pTZ18U RNA were used as nonspecific competitors. The arrows show free RNAs (F) and RNA-protein complexes (C). P, no cellular extract; (−), no unlabeled competitors.

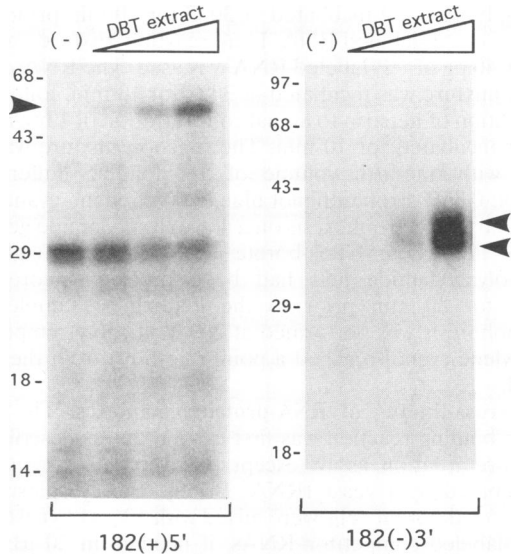

FIG. 4. UV cross-linking of RNA-protein complexes. ^{32}P-labeled 182(+)5′ RNA mixed with 2.2, 5.0, or 7.2 μg of cellular extracts and 182(−)3′ RNA mixed with 1.0, 3.0, or 6.0 μg of cellular extracts were UV irradiated, digested with RNase, and separated by SDS-PAGE on 12.5% polyacrylamide gels. Arrowheads indicate the 55-kDa and 35- and 38-kDa proteins which cross-linked to the 182(+)5′ and 182(−)3′ RNAs, respectively. In (−) lanes, no cellular extracts were added. The numbers on the left side show the sizes (in kilodaltons) of standard protein markers.

unstable protein, because it was detected only with fresh cellular extracts. Similar UV cross-linking studies were performed with 90(+)3′ RNA; no proteins were detected (data not shown). This finding is consistent with the results of the gel-retardation assay (Fig. 2).

To examine the specificity of UV cross-linking reactions, the unlabeled homologous RNAs were used as specific competitors, and RNA transcribed from plasmid pTZ18U was used as a nonspecific competitor. As shown in Fig. 5, when increasing amounts of the specific competitors were used, the amounts of the 55-, 35-, and 38-kDa proteins cross-linked to both RNAs decreased proportionally; in contrast, comparable amounts of the vector pTZ18U RNA did not reduce the amounts of the cross-linked proteins (Fig. 5). These data showed that the binding of 182(+)5′ and 182(−)3′ RNAs to these cellular proteins was specific. In contrast, the amount of the 29-kDa band was not reduced by either the specific or nonspecific competitor RNAs.

Mapping of the protein-binding sites on 182(+)5′ and 182(−)3′ RNAs. To localize the binding sites of the cellular proteins on the MHV UTR RNAs, truncated RNAs of different sizes were transcribed from the different DNA templates which had been digested at different restriction sites (Fig. 1). The transcribed RNAs were cross-linked to the cellular proteins by UV irradiation and digested with RNase. As shown in Fig. 6A, roughly the same amounts of the 55-kDa protein were cross-linked to both 112(+)5′ and 182(+)5′ RNAs; in contrast, 56(+)5′ RNA was not cross-linked to the protein. These results indicated that the 56-nt region between nt 56 and 112 from the 5′ end of the genomic RNA was crucial for the binding of the 55-kDa protein or was the actual protein-binding site. It is notable that UV irradiation of these RNAs, particularly 112(+)5′ RNA, in the absence of cellular extracts generated multiple RNA bands which decreased in amount when cellular extracts were added. These multiple bands probably represent RNase-resistant RNA fragments formed by UV cross-linking of secondary structures, because a single RNA band was detected when RNA transcripts without UV irradiation were analyzed by denaturing agarose gel electrophoresis (data not shown). The use of both RNase A and RNase T1 for this experiment did not alter the RNA patterns.

The mapping experiments with the 3′ end of the negative-strand RNA showed that the 35- and 38-kDa proteins were cross-linked to the 126(−)3′ RNA more efficiently than to the

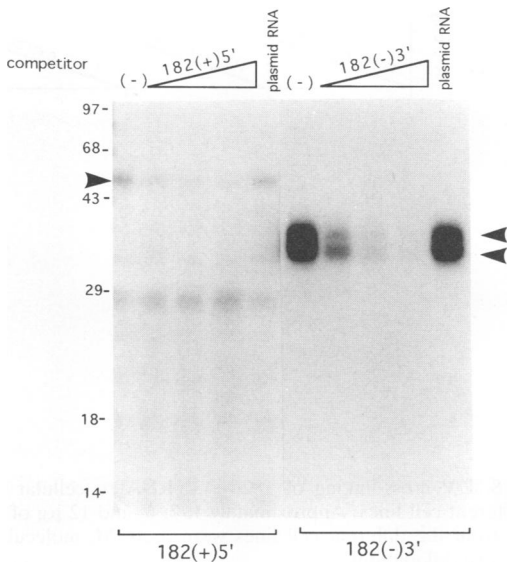

FIG. 5. Competition assays of UV cross-linking. Cellular extracts were first incubated with various amounts of unlabeled 182(+)5′ or 182(−)3′ RNAs or plasmid pTZ18U RNAs for 10 min and then were incubated with the respective ^{32}P-labeled RNAs. The unlabeled RNAs used represented 80-, 160-, or 320-fold excess of the same labeled RNAs, while plasmid RNA represented 160-fold molar excess. Arrowheads show the 55-kDa and 35- and 38-kDa proteins cross-linked to 182(+)5′ and 182(−)3′ RNAs, respectively. In (−) lanes, no competitor RNA was added. The sizes (in kilodaltons) of the standard protein markers are indicated on the left side.

182(−)3′ RNA; in contrast, 70(−)3′ was not cross-linked to those proteins (Fig. 6B). These results indicated that the binding site of the 35- and 38-kDa proteins on the 3′-end-negative-strand RNA are in the 56-nt region between nt 56 and 112 from the 3′ end of the negative-strand RNA. This region represents the complementary region of the 55-kDa protein-binding site on the positive-strand RNA (see Fig. 1). These RNAs also generated multiple RNase-resistant RNA fragments in the absence of cellular extracts; their amounts decreased when increasing amounts of cellular extracts were added. Thus, they are likely derived from the cross-linked RNA secondary structures. The results of UV cross-linking studies on both positive- and negative-strand RNAs thus indicated that at least three cellular proteins bind to the same site on the complementary strands near the 5′ end of MHV genomic RNA.

Binding of the 55-kDa protein to longer RNA transcripts. Because the RNA transcripts used in the experiments described above contained vector sequences and represented only a small fraction of the full-length MHV viral genomic RNA, it is possible that the conformation of these RNA transcripts is different from that of the full-length RNA molecules. Therefore, the RNA-binding proteins described above may not bind to the natural viral RNAs. To rule out this possibility, we used 681-nt and 1,182-nt transcripts of DE25 plasmid (20), which contain only one extra G residue at the 5′ end of the positive-strand RNA transcripts, for UV cross-linking studies. Figure 7 shows that the 55-kDa protein was cross-linked to both RNAs. We conclude that this protein likely binds to the natural MHV viral RNA and that the vector sequences did not contribute to the protein binding. Furthermore, no other proteins were cross-linked to these two RNAs. Thus, within the nearly 1.2 kb of the 5′ end of positive-strand RNA, only the 5′-end UTR is capable of binding cellular proteins.

UV cross-linking studies of 182(−)3′ RNA with cellular extracts from different cell lines. For the binding studies described above, the cellular extracts from DBT cells were used, because these cells were highly susceptible to MHV infection (9). To determine whether the proteins bound to MHV UTR RNAs are conserved among different cell lines, 182(−)3′ RNA was also cross-linked to the cellular extracts derived from HeLa cells and COS-7 cells. As shown in Fig. 8, the 35-kDa protein was detected in all three cell lines, whereas the 38-kDa protein was barely detectable in HeLa or COS-7 cell extracts. This result shows that the 38-kDa protein is not expressed, or is expressed in very small amounts, in these two cell lines, while the 35-kDa protein is expressed in all of the cell lines.

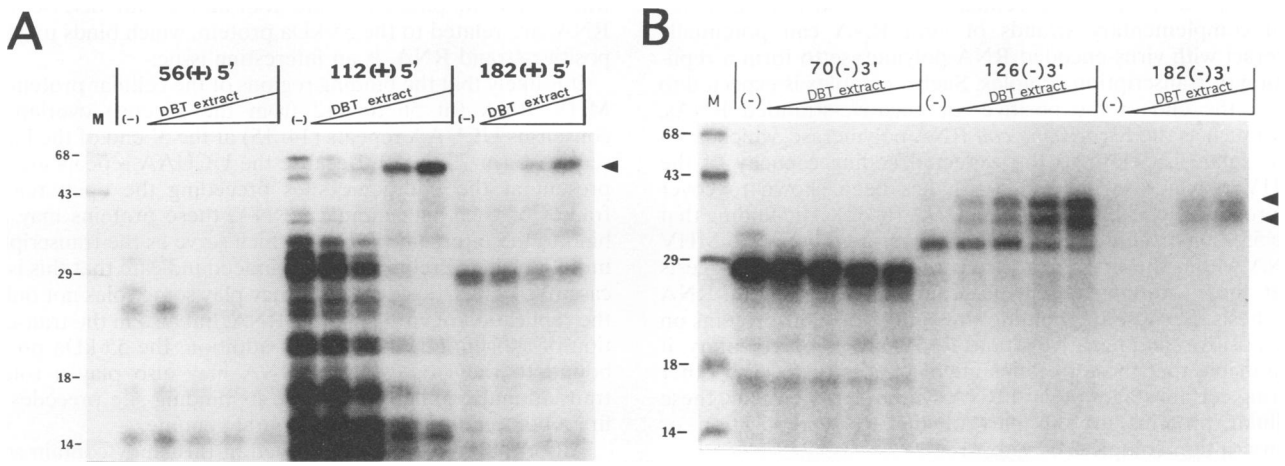

FIG. 6. Mapping of the binding sites of cellular proteins on 5′-end-positive-strand (A) and 3′-end-negative-strand (B) MHV RNAs. Various amounts (0.7 to 7.2 μg in panel A and 0.9 to 7.2 μg in panel B) of the cellular extracts were mixed with ^{32}P-labeled RNAs and UV irradiated. Arrowheads show the 55-kDa protein (A) and the 35- and 38-kDa proteins (B). In (−) lanes, no cellular extracts were added. M, molecular mass standards (in kilodaltons).

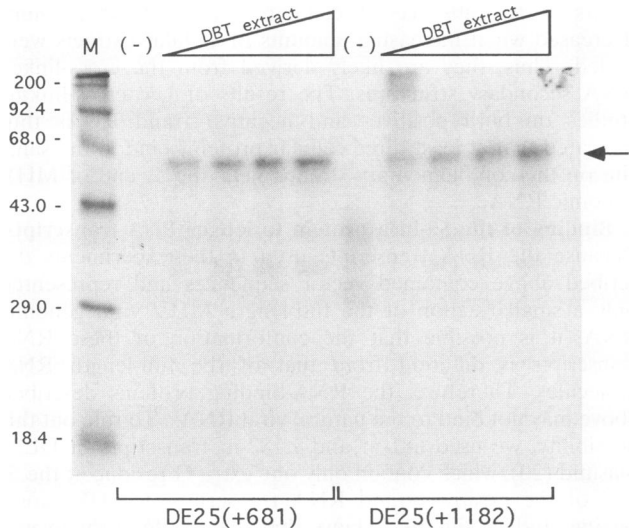

FIG. 7. UV cross-linking studies of long RNA transcripts. DE25 plasmid (20) was digested with *Eag*I and *Afl*II and transcribed with T7 RNA polymerase to yield 681- and 1,182-nt RNAs, respectively, which represent 5′-end-positive-strand RNA fragments with only 1 extra nucleotide. UV cross-linking studies were performed with 3.5, 5.8, or 11.5 μg of DBT cellular extracts. In (−) lanes, no cellular extracts were added. The arrow indicates the 55-kDa band. M, molecular mass standards (in kilodaltons).

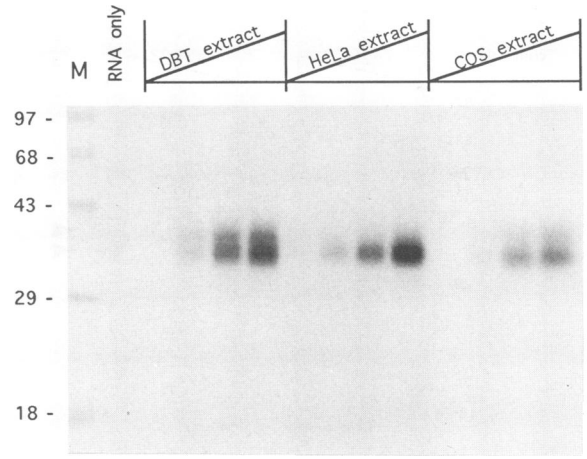

FIG. 8. UV cross-linking of 182(−)3′ RNA to cellular extracts from different cell lines. Approximately 1, 3, 6, and 12 μg of cellular extracts from the different cell lines were used. M, molecular mass standards (in kilodaltons).

DISCUSSION

In this report, we have shown that several cellular proteins of different sizes bind to the different strands of MHV RNAs in the region corresponding to the 5′ end of positive-strand genomic RNA and the 3′ end of negative-strand cRNAs. Interestingly, these proteins bind to the complementary sites of the same 56-nt region near the ends of both positive- and negative-strand RNAs. The nature and functions of these cellular proteins are still not clear; however, the fact that the binding sites of these proteins are located near the end of the viral genomic and cRNAs suggests that they may be involved in RNA replication or transcription, because RNA replication is expected to start from the ends of viral RNA, and the 5′-leader RNA has been shown to be involved in subgenomic mRNA transcription (14). These cellular proteins on both genomic and complementary strands of viral RNA can potentially interact with virus-encoded RNA polymerase to form a replication or transcription complex. Such a complex is expected to cover the end of the positive- or negative-stranded RNAs, inasmuch as the *Escherichia coli* RNA polymerase, which has a molecular size close to the expected coding capacity of the MHV polymerase gene (14, 16), has been shown to cover approximately 75 bp of template DNA (6, 32). The finding that the 55-kDa protein is the only cellular protein bound to MHV RNA within the first 1.2 kb from the 5′ end further suggests that these proteins are involved in the initiation of RNA synthesis. Because the binding sites of the cellular proteins on the positive- and negative-strand RNAs are complementary, it is possible that these proteins might interact with each other during certain stages of viral RNA synthesis. Potentially, these cellular proteins are all part of the RNA replication or transcription complexes.

It is interesting that no cellular proteins were found to bind to the 3′ end of positive-strand genomic RNA. In MHV-infected cells, the incoming viral genomic RNA is expected to be replicated from the 3′ end of positive-strand RNA into negative-strand RNA by virus-specific RNA polymerase. Thus, single-stranded, positive-sense genomic RNA likely serves directly as the template for the synthesis of negative-strand RNA. The simplicity of this template may minimize the need for cellular factors to participate in RNA replication.

Several cellular proteins have been reported to bind to RNA fragments representing UTR RNA or its complementary strand from other RNA viruses. For example, the 3′ end of the Sindbis virus negative-strand RNA, which is thought to be a promoter for RNA replication, was cross-linked to cellular proteins 42, 44, and 52 kDa in size by UV irradiation (24). The 5′-UTR RNA of poliovirus was reported to be cross-linked to a 54-kDa cellular protein, which may be a common translation factor for viral and nonviral mRNAs (7). Other cellular proteins with sizes of 48 and 38 kDa were also cross-linked to other sites on the 5′-UTR RNA and may be associated with specific poliovirus translation (7). A 57-kDa cellular protein was found to cross-link to two sites in the internal ribosomal entry site on the 5′-UTR of foot-and-mouth-disease virus RNA (18). Whether the 54- and 57-kDa cellular proteins, which bind to poliovirus and foot-and-mouth disease virus RNA, are related to the 55-kDa protein, which binds to MHV positive-strand RNA, is an interesting issue.

It is likely that the binding regions of the cellular proteins on MHV RNA (nt 56 to 112 from the 5′ end) overlap the consensus UCUAA repeats (14, 15) at the 3′ end of the leader sequence (nt 70 to 80). Because the UCUAA repeats are also present at the intergenic sites preceding the open reading frames of each subgenomic mRNA, these proteins may also bind to the intergenic regions, which serve as the transcription initiation sites. Preliminary data indeed indicate that this is the case (35). Thus, these proteins may play some roles not only in the replication of viral genomic RNA, but also in the transcription of subgenomic mRNAs. In addition, the 55-kDa protein bound to the viral genomic RNA may also play a role in translational regulation, because its binding site precedes the first open reading frame in the viral genome.

All of the RNA transcripts used in this study contain some vector sequences, and some of them contain an extra T7 promoter sequence. However, among the 5′-end-positive-strand RNA fragments used, 56(+)5′ RNA did not cross-link to the 55-kDa protein, although it contains the same vector and

extra T7 promoter sequence as those in 112(+)5′ and 182(+)5′. Furthermore, a long (1.2-kb) RNA fragment without the vector sequence bound the same 55-kDa protein. Similarly, among the 3′-end-negative-strand RNA fragments used, 70(−)3′ RNA did not cross-link to the 35- and 38-kDa proteins although it contains the same vector sequences as those in 126(−)3′ and 182(−)3′ RNAs. Therefore, these extra sequences were not responsible for the specific bindings observed between the MHV UTR RNAs and the cellular proteins, and these cellular proteins likely bind to the full-length viral RNAs in the virus-infected cells.

The 35-kDa protein, which bound to the 3′ end of negative-strand RNA, is present in all three of the cell lines studied. It has been shown that MHV can replicate in COS-7 cells after transfection of MHV genomic RNA, even though COS-7 cells are not naturally susceptible to MHV infection because of the lack of an MHV receptor (34). Thus, COS-7 cells should contain factors needed for MHV replication, and the 35-kDa protein may be one of these factors. In contrast, the 38-kDa protein was not detected in either COS-7 or HeLa cells; it may have a role different from that of the 35-kDa protein and is not necessary for viral RNA replication. The relationship between the 35- and 38-kDa proteins is not clear. The 38-kDa protein may represent the posttranslational modification product of the 35-kDa protein.

The UV cross-linking studies, especially those with 112(+)5′ and 56(+)5′ RNAs, detected several RNase-resistant RNA bands, which decreased in amount upon the addition of cellular extracts (Fig. 6A). These bands likely represent RNA fragments with strong secondary structures. Thus, these findings suggest that cellular extracts contain some enzymatic activities, such as RNA helicases, which reduced the secondary structures of RNAs and rendered them sensitive to RNase digestion. RNA helicase activities in some proteins, such as eukaryotic initiation factor 4A (eIF-4A) (27, 28), human p68 protein (10), and RNA helicases from HeLa cell nuclear extracts (3), have previously been detected. Whether the proteins detected in this study have RNA helicase activities will require additional studies.

REFERENCES

1. **Andino, R., G. E. Rieckhof, and D. Baltimore.** 1990. A functional ribonucleoprotein complex forms around the 5′ end of poliovirus RNA. Cell **63**:369–380.
2. **Baric, R. S., S. A. Stohlman, and M. M. C. Lai.** 1983. Characterization of replicative intermediate RNA of mouse hepatitis virus: presence of leader RNA sequences on nascent chains. J. Virol. **48**:633–640.
3. **Claude, A., J. Arenas, and J. Hurwitz.** 1991. The isolation and characterization of an RNA helicase from nuclear extracts of HeLa cells. J. Biol. Chem. **266**:10358–10367.
4. **Compton, S. R., D. B. Rogers, K. V. Holmes, D. Fertsch, J. Remenick, and J. J. McGowan.** 1987. In vitro replication of mouse hepatitis virus strain A59. J. Virol. **61**:1814–1820.
5. **Dildine, S. L., and B. L. Semler.** 1992. Conservation of RNA-protein interactions among picornaviruses. J. Virol. **66**:4364–4376.
6. **Galas, D. J., and A. Schmitz.** 1978. DNase footprinting: a simple method for the detection of protein-DNA binding specificity. Nucleic Acids Res. **5**:3157–3170.
7. **Gebhard, J. R., and E. Ehrenfeld.** 1992. Specific interactions of HeLa cell proteins with proposed translation domains of the poliovirus 5′ noncoding region. J. Virol. **66**:3101–3109.
8. **Gluzman, Y.** 1981. SV40-transformed simian cells support the replication of early SV40 mutants. Cell **23**:175–182.
9. **Hirano, N., K. Fujiwara, S. Hino, and M. Matumoto.** 1974. Replication and plaque formation of mouse hepatitis virus (MHV-2) in mouse cell line DBT culture. Arch. Gesamte Virusforsch. **44**:298–302.
10. **Hirling, H., M. Scheffner, T. Restle, and H. Stahl.** 1989. RNA helicase activity associated with the human p68 protein. Nature (London) **339**:562–564.
11. **Joo, M., and S. Makino.** 1992. Mutagenic analysis of the coronavirus intergenic consensus sequence. J. Virol. **66**:6330–6337.
12. **Konarska, M. M., and P. A. Sharp.** 1986. Electrophoretic separation of complexes involved in the splicing of precursors to mRNA. Cell **46**:845–855.
13. **Laemmli, U. K.** 1970. Cleavage of structural proteins during the assembly of the head of bacteriophage T4. Nature (London) **227**:680–685.
14. **Lai, M. M. C.** 1990. Coronavirus: organization, replication and expression of genome. Annu. Rev. Microbiol. **44**:303–333.
15. **Lai, M. M. C., C. D. Patton, R. S. Baric, and S. A. Stohlman.** 1983. Presence of leader sequences in the mRNA of mouse hepatitis virus. J. Virol. **46**:1027–1033.
16. **Lee, H.-J., C.-K. Shieh, A. E. Gorbalenya, E. V. Koonin, N. La Monica, J. Tuler, A. Bagdzhadzhyan, and M. M. C. Lai.** 1991. The complete sequence (22 kilobases) of murine coronavirus gene 1 encoding the putative proteases and RNA polymerase. Virology **180**:567–582.
17. **Lin, Y.-J., and M. M. C. Lai.** 1993. Deletion mapping of a mouse hepatitis virus defective interfering RNA reveals the requirement of an internal and discontiguous sequence for replication. J. Virol. **67**:6110–6118.
18. **Luz, N., and E. Beck.** 1991. Interaction of a cellular 57-kilodalton protein with the internal translation initiation site of foot-and-mouth disease virus. J. Virol. **65**:6486–6494.
19. **Makino, S., and M. Joo.** 1993. Effect of intergenic consensus sequence flanking sequences on coronavirus transcription. J. Virol. **67**:3304–3311.
20. **Makino, S., and M. M. C. Lai.** 1989. High-frequency leader sequence switching during coronavirus defective interfering RNA replication. J. Virol. **63**:5285–5292.
21. **Makino, S., C.-K. Shieh, L. H. Soe, S. C. Baker, and M. M. C. Lai.** 1988. Primary structure and translation of a defective interfering RNA of murine coronavirus. Virology **166**:550–560.
22. **Niesters, H. G. M., and J. H. Strauss.** 1990. Defined mutations in the 5′ nontranslated sequence of Sindbis virus RNA. J. Virol. **64**:4162–4168.
23. **Pachuck, C. J., P. J. Bredenbeek, P. W. Zoltick, W. J. M. Spaan, and S. R. Weiss.** 1989. Molecular cloning of the gene encoding the putative polymerase of mouse hepatitis coronavirus, strain A59. Virology **171**:141–148.
24. **Pardigon, N., and J. H. Strauss.** 1992. Cellular proteins bind to the 3′ end of Sindbis virus minus-strand RNA. J. Virol. **66**:1007–1015.
25. **Perlman, S., D. Ries, E. Bolger, L. J. Chang, and C. M. Stoltzfus.** 1986. MHV nucleocapsid synthesis in the presence of cycloheximide and accumulation of negative strand MHV RNA. Virus Res. **6**:261–272.
26. **Pogue, G. P., and T. C. Hall.** 1992. The requirement for a 5′ stem-loop structure in brome mosaic virus replication supports a new model for viral positive-strand RNA initiation. J. Virol. **66**:674–684.
27. **Ray, B. K., T. G. Lawson, J. C. Kramer, M. H. Cladaras, J. A. Grifo, R. D. Abramson, W. C. Merrick, and R. E. Thach.** 1985. ATP-dependent unwinding of messenger RNA structure by eukaryotic initiation factors. J. Biol. Chem. **260**:7651–7658.
28. **Rozen, F., I. Edery, K. Meerovitch, T. E. Dever, W. C. Merrick, and N. Sonenberg.** 1990. Bidirectional RNA helicase activity of eucaryotic translation initiation factors 4A and 4F. Mol. Cell. Biol. **10**:1134–1144.
29. **Schreiber, E., P. Matthias, M. M. Müller, and W. Schaffner.** 1989. Rapid detection of octamer binding proteins with 'mini-extracts', prepared from a small number of cells. Nucleic Acids Res. **17**:6419.
30. **Shieh, C.-K., L. H. Soe, S. Makino, M. F. Chang, S. A. Stohlman, and M. M. C. Lai.** 1987. The 5′-end sequence of the murine coronavirus genome: implications for multiple fusion sites in leader primed transcription. Virology **156**:321–330.
31. **Spaan, W., H. Delius, M. Skinner, J. Armstrong, P. Rottier, S. Smeekens, B. A. M. van der Zeijst, and S. G. Siddell.** 1983.

Coronavirus mRNA synthesis involves fusion of noncontiguous sequences. EMBO J. **2:**1839–1844.
32. **von Hippel, P. H., D. G. Bear, W. D. Morgan, and J. A. McSwiggen.** 1984. Protein-nucleic acid interactions in transcription: a molecular analysis. Annu. Rev. Biochem. **53:**389–446.
33. **Yokomori, K., L. R. Banner, and M. M. C. Lai.** 1991. Heterogeneity of gene expression of the hemagglutinin-esterase (HE) protein of murine coronaviruses. Virology **183:**647–657.
34. **Yokomori, K., and M. M. C. Lai.** 1992. Mouse hepatitis virus utilizes two carcinoembryonic antigens as alternative receptors. J. Virol. **66:**6194–6199.
35. **Zhang, X.-M., and M. M. C. Lai.** 1992. Unpublished observation.